Recent Achievements with a Cryogenic Ultra-lightweighted HB-Cesic® Mirror

By Matthias R. Krödel[1)], Peter Hofbauer[1)],
Christophe Devilliers[2)], Zoran Sodnik[3)], Patrick Robert[4)]

[1)] ECM Ingenieur-Unternehmen für Energie- und Umwelttechnik GmbH, Ridlerstr. 31d,
D-80339 Munich, Germany
[2)] Thales Alenia Space, 100, Boulevard du Midi, BP 99, F-06156 Cannes la Bocca Cedex, France
[3)] ESA, ESTEC Keplerlaan 1, PO Box 299, 2200 AG Noordwijk ZH, The Netherlands
[4)] SESO, Pôle d'activité d'Aix Les Milles, 305 rue Louis Armand, CS 30504, 13593 Aix en
Provence Cedex 3, France

ABSTRACT

During the past two years, ECM, Germany, together with Mitsubishi Electric Corporation (MELCO), Japan, developed a new carbon-fiber-reinforced SiC material, called HB-Cesic®, which possesses superior mechanical and thermal cryogenic properties compared to traditional Cesic®. This combination makes HB-Cesic® an excellent choice for large cryogenic mirrors, which will be required for future scientific space missions, such as SPICA and DARWIN.

ESA contracted Thales Alenia Space (TAS), France, to design a super-lightweighted HB-Cesic® mirror with a diameter of 600 mm, isostatic fixations, and a special astigmatism compensation device (ACD) for mirror shape control. The mirror was manufactured by ECM, polished and coated by Société Européenne de Systèmes Optiques (SESO), France, and tested to cryogenic temperatures by TAS. The measured wave-front error at ambient and cryogenic temperatures demonstrated the excellent homogeneity of HB-Cesic® and TAS' expertise in mirror mounting. Furthermore, when thermally actuated, the ACD exhibited perfect control of the mirror shape.

This success confirmed HB-Cesic®'s superior material properties and its applicability to future cryogenic space mirrors.

In this paper we describe the design and fabrication process of this cryogenic mirror and give test results at ambient and cryogenic temperatures.

Keywords: **Cesic®, Ceramic mirrors, Cryogenic performance**

1. INTRODUCTION

Future scientific space missions require ever more demanding large optics that work at cryogenic temperatures. In the frame of a Darwin assessment study conducted under ESA contract by TAS, the need of future very lightweight cryogenic mirrors with superior optical quality has been recommended; and detailed requirements have been established. For instance, such mirrors need to be of sizes up to 3.5 m in diameter, with a mass of less than 250 kg corresponding to an areal density of less than 25 kg/m^2 and possess excellent optical quality at cryogenic temperature down to 40 K.

Furthermore, as part of the Darwin assessment study, TAS studied in depth the non-planar Emma configuration, which is composed of three large free-flying receiver mirrors and a central beam combiner on which the light from the receiver mirrors converges. The mirrors create a "virtual" parabola, called the synthesis telescope. The optical integrity of the evolutionary synthesis telescope is ensured by a continual adjustment of the astigmatism and radius of curvature of each of the three receiver mirrors.

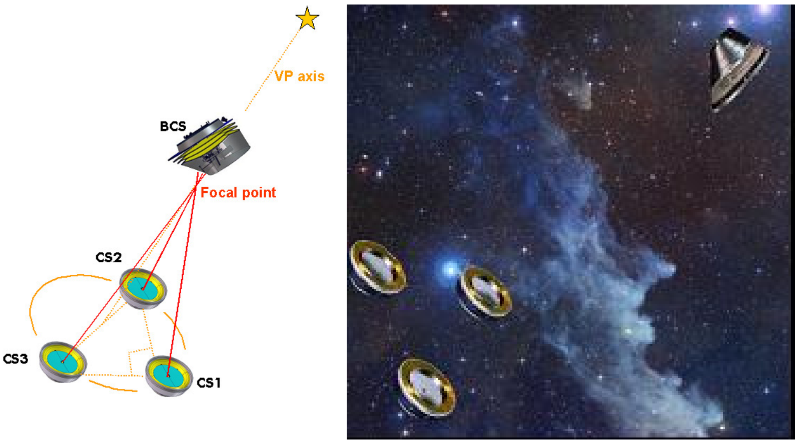

Figure 1. Darwin free flyer interferometer telescope with mirrors up to 3.5 m in diameter.

Moreover, there are a number of other foreseen missions that also require large, very lightweight, and ultrastable mirrors and optical benches, such as the SPICA, Euclid and FIRI missions.

On this basis, ESA contracted Thales Alenia Space (TAS) for a technology research project, with the following objectives:

- Conduct an in-depth review of the requirements of future ultrastable lightweight optical systems;
- evaluate potential trade-off technologies that meet such requirements;
- design and establish the performance of large receiver mirrors based on the Darwin mission requirements; and
- design, manufacture, and test a representative optical demonstrator mirror to validate its optical stability under cryogenic conditions, including a system to correct astigmatism.

TAS selected ECM's HB-Cesic® optical material for its unique material properties, such as a high specific Young modulus, high thermal conductivity, low CTE, and high strength (especially for a ceramic), and its versatile manufacturing capabilities, which allow manufacturing large monolithic structures from a single homogenous greenbody blank.

First an ultra-lightweighted technological (ULT) mirror was designed, with a 600-mm diameter, made of HB-Cesic®, and possessing a mass of just 5 kg. The mirror has also its isostatic fixations and a special astigmatism compensation device (ACD) for mirror shape control. Furthermore, this mirror system needs to be of high optical quality, compatible with cryogenic temperatures, and able to withstand launch loads. The Invar fixation design needs to be optimized with respect to mounting interface biases, representative launch loads, and cool-down to cryo-temperatures in order to minimize wave front errors (WFE).

Upon completion of the design, the mirror was manufactured by ECM, polished by SESO, and then tested from ambient to cryogenic temperatures by TAS.

The surface quality of the polished HB-Cesic® mirror was then validated by SESO, with particular attention paid to quilting print-through effects. The gravity impact on the WFE was measured; and the fixation locations of the mounts were optimized to minimize gravity effects.

After polishing the mirror to a surface figure error of less than 20 nm RMS, it was optically tested between ambient and cryogenic temperatures.

The integrated ACD system was then installed on the mirror and activated at cryo temperatures. The WFE change was measured during the integration of the ACD system and its performance was measured under cryogenic conditions.

2. DESIGN OF THE ULTRA-LIGHTWEIGHTED TEST MIRROR

The ULT mirror design was optimized to be representatively scaled from the Emma/SPICA flight mirrors. ULT mirror had an external diameter of 600 mm and was constructed of HB-Cesic® with a face sheet thickness 3 mm, strengthened by a rib pattern with ribs thickness of 1.2 to 1.5 mm. The mirror was polished directly on bare HB-Cesic®, to validate surface roughness performance for future space missions, and gold coated, to determine impact of gold layer on thin HB-Cesic® face sheet . The mirror I/F fixations was fully representative of flight fixation I/F.

The ACD beam, also to be constructed of HB-Cesic®, allows the adjustment in a single direction of the mirror's astigmatism at 100 K and is a flight demonstration concept. The ACD beam is mounted firmly on the back of the ULT mirror via two Invar interfaces as illustrated in Fig. 3. By either heating or cooling the beam, the length is either increased or decreased microscopically by ± DL/L. It is these length changes that create changes in the mirror's astigmatism. With just one ACD beam, these changes occur in just one direction. In future flight mirrors, two ACD beams will be used to create changes in two perpendicular directions.

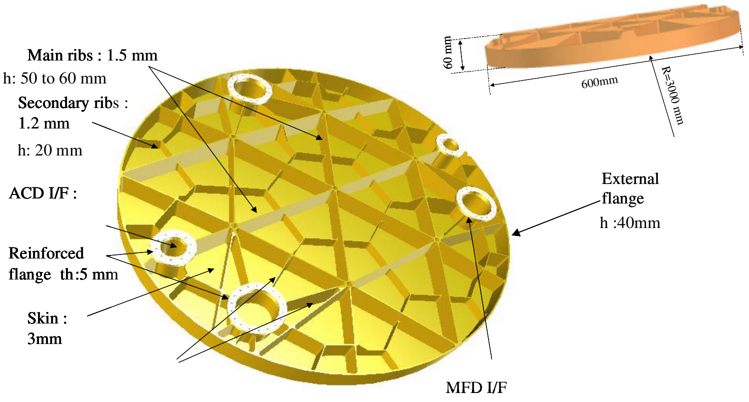

Figure 2. The ULT mirror design.

The mirror fixation filtering devices have been optimized vs. eigenfrequency, loads, I/F filtering capability, and cryogenic impact in order to stabilize the ULT mirror. The optimization was accomplished by the development of special cryogenic fixation devices. However, the CTE mismatch between glue and HB-Cesic® remains a significant contributor to the mirror WFE at cryo temperatures, especially for such an ultra-lightweighted mirror.

After assembly of the ACD beam to the mirror, the mirror was integrated to an Invar frame, which constitutes the interface with the cryo chamber.

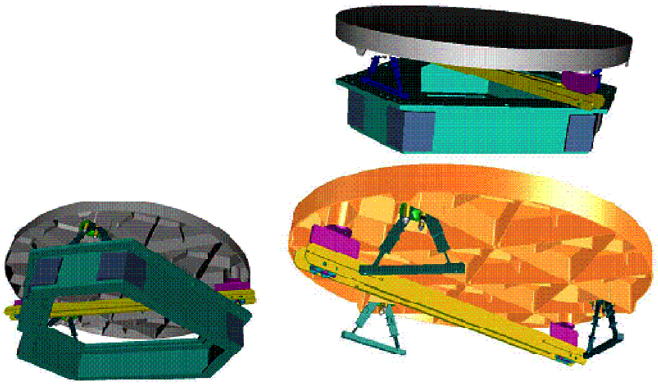

Figure 3. Mirror on its Invar frame.

The mass of the 600-mm mirror is less than 5 kg and corresponds to an areal density of 17.8 kg/m^2.

The ULT mirror performance was assessed via detailed FE analyses, using a model with 1,400,000 nodes and 950,000 elements.

This detailed modeling was necessary to assess the optical performance vs. all nm-scale disruptive, especially at high frequencies.

Analysis of the mirror's mechanical performance show large safety margins compared to the requirements. For instance, the first eigenfrequency is 135 Hz, which exceeds by far the required frequency of 50 Hz.

The strength under a 25-g load in the X, Y, and Z directions was demonstrated by FEM calculations, showing that the mirror has high safety margins compared to the allowable stresses for the HB-Cesic® material.

The ULT mirror optical performance was computed via detailed opto-thermo-elastic modeling for numerous load cases to demonstrate the WFE performance at cryo temperatures with and without the ACD beam.

The mirror's opto-mechanical performance under gravity loads was also computed, with gravity acting along the X and Z axes and for different I/F displacements.

3. FABRICATION OF THE MIRROR

ECM received from Thales Alenia Space the design file for the ULT mirror and the order to start the fabrication. One of the main challenges was to fabricate the very thin and rather long ribs. Since this was the first time that ECM was confronted by such a challenge, milling parameters were optimized first during greenbody fabrication. Then, before the start of the actual fabrication of the mirror, we performed some mock-up testing in order to determine whether we had to tailor the Si-infiltration process to the specific design of the mirror or could use our standard process, developed for Cesic® optics components in the past.

Fig. 4 shows the mock-up both in the greenbody stage, and after its successful infiltration - Fig. 5. In order to evaluate the performance of the infiltrated mock-up and, in particular, its homogeneity, was performed first a visual inspection and then cut out random sections of the ribs for further microstructure inspections – also illustrated in Fig. 5. The result of the microstructure inspection was excellent.

Figure 4 Mock-up greenbody (C/C)

Figure 5 Mock-up infiltrated with samples cutouts

After a fully successful evaluation of the infiltration of the mock-up, including the ribs, we started the greenbody fabrication of the actual 600-mm mirror. Due to the fact that this mirror will operate at cryogenic temperatures, we took particular care during the inspection of the raw material to ensure its homogeneity in order to be confident of the thermal stability of the final mirror performance. For this characterization, we took many random samples from different locations of the raw material and used them as witness samples during the fabrication process.

Due to the ribs' thickness of just 1.2 to 1.5 mm, another major challenge in the manufacturing process was to obtain a final shape of the mirror surface that corresponded to the nominal design shape.

After infiltration, we measured the shape of the mirror surface and determined that the maximum deviation from the nominal shape was 0,38 mm P-V, which we consider to be excellent. This result confirmed that the uncertainty of the shrinkage factor, between greenbody dimensions and final, fully infiltrated HB-Cesic® structure, is very small with a value of just 0.05%. A low shrinkage is also of advantage in producing the optimal oversize of mirrors for grinding after infiltration, in order to correct the mirror shape to the specified radius of curvature.

After completion of the visual inspection after infiltration, ECM performed the final machining of the mirror in preparation of the interfaces for the mounts and the mirror surface for polishing.

Due to the fact that HB-Cesic® can be machined by using EDM (Electrical Discharge Machining), we were able to cut the injection holes for the gluing of the Invar inserts directly inside the mounts.

Finally, the grinding of the mirror with conventional grinding tools was fast and successful. After just three weeks, the mirror shape was corrected from the original 0.38 mm down to 20 µm P-V.

After pre-grinding and preparation of the interface, the mirror was sent for polishing to SESO.

4. POLISHING OF THE TEST MIRROR

The polishing of the ULT mirror started with the pre-machined greenbody substrate delivered by ECM to SESO. At this level the optical surface deviation from the theoretical sphere was 20 µm P-V.

The different steps performed by SESO were the following:

- Grinding: This abrasion process allowed lowering the deviation between the measured surface and the theoretical shape to below 3µm P-V.
- Fine grinding: This intermediate step allowed lowering the surface error down to about 1 µm P-V, while starting to get a polished surface.
- Rough polishing: At this level, the mirror was still being polished on its full face at once, and the abrasives we used were getting smaller in grain size. The actual stop criterion was about 50 nm RMS.
- Gluing of the Mirror Fixing Devices (MFD) pads onto the mirror and assembly on the Invar frame: This step was in preparation for the final polishing activities to allow correction of mounting artifacts. SESO participated in the design of the MFDs and Pads to minimize any effects due to the mounting/dismounting activities and to the cryo/ambiance testing sequence at TAS.
- Polishing with the Computer Controlled Polishing Machine (CCPM): This step continued until we achieved the required surface accuracy and micro-roughness.
- Dismounting of the Invar frame for coating of the mirror.
- Coating of the mirror (equipped with MFDs) with a hard gold coating: The purpose of the hard gold coating was to protect the mirror surface during cleaning.
- Remounting of the mirror on the Invar frame, followed by delivery to TAS.

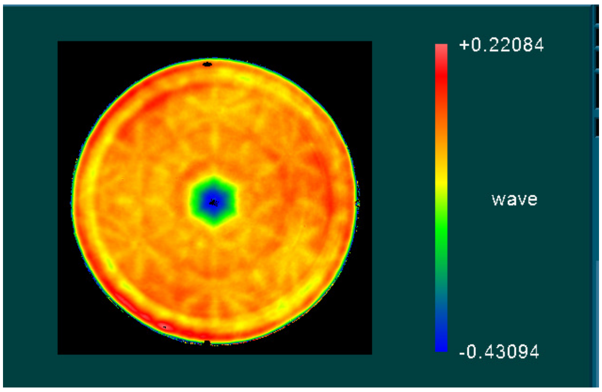

Figure 6. Inspection of the mirror SFE (Surface error) after rough polishing to 48.106 nm RMS.

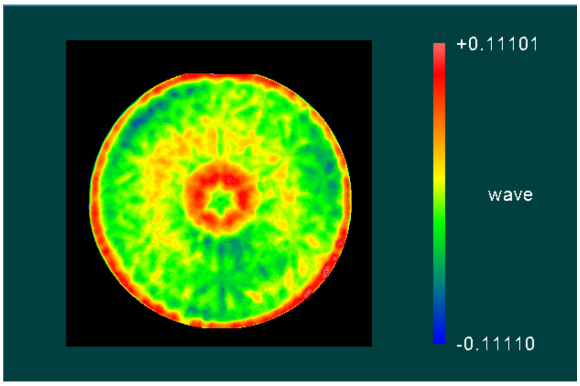

Figure 7. Inspection of the mirror SFE after MFDs gluing, frame mounting, and final polishing – 20.1809 nm RMS.

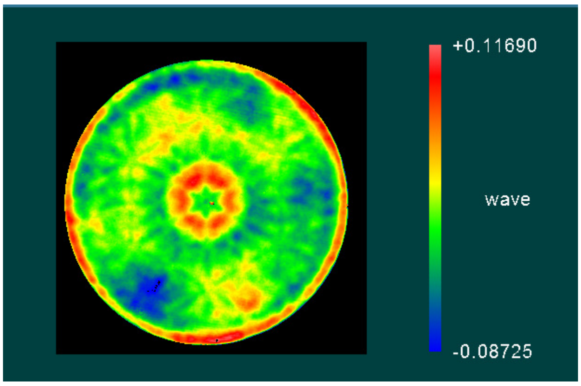

Figure 8. Mirror SFE after coating and remounting –20.445 nm RMS.

We had to deal with numerous challenges in the steps just enumerated:
The main issue of the full-face activities was to avoid generating any quilting effect (also called "print-through") due to the extreme light-weighting design. The achieved result was satisfactory and allowed us to get down to the required level for CCPM polishing.

The main concern of the MFDs mounting optimization was to minimize the gravity effects during inspection at ambient conditions. The optimization was achieved thanks to shims inserted between MFDs caps and Pads cemented inside the mirror housing. The gluing of the pads and the mounting on the frame were done before final polishing to be able to compensate during polishing for any possible effects linked to mounting stresses.

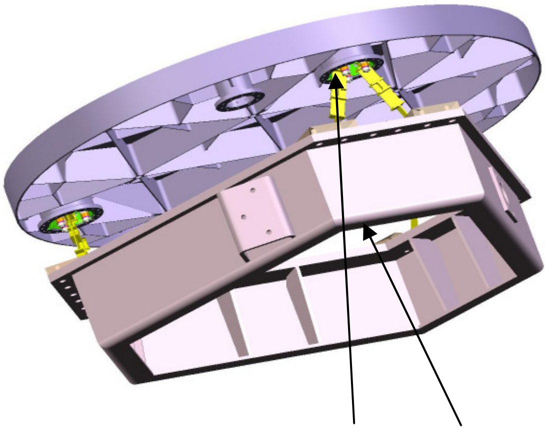

Figure 9. Mirror mounted with MFDs and Invar frame.

The principal issue of CCPM polishing was the removal rate, due to the use of a very localized polishing tool. We dealt with this issue by the following method: While the diameter of the tool was reduced, we lowered the removal rate accordingly.

To avoid losing too much in rate removal, SESO optimized the polishing compound and its management during the polishing process, the polishing tool support to allow a good removal rate, and the polishing pressure and tool speed to avoid generating quilting during CCPM polishing.

Regarding the WFE measurements the main concern was to be able to get consistent measurement results before MFDs mounting (mirror measured free, held within the MFDs pads housings) and after MFDs pads gluing and mounting on the interface frame. We were successful in carrying out these measurements thanks to the supporting options taken in both cases – i.e., the deviations were within the measurement accuracy in both set-ups.

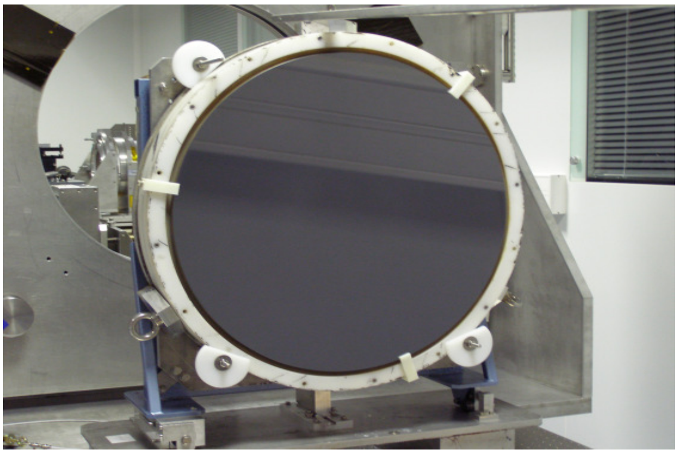

Figure 10. Mirror on its support during inspection measurements.

The final challenge was the gold coating, which we solved by coating the mirror with mounted MFDs (even though the interface frame was dismounted), avoiding stresses on the mirror and thereby generating major WFE evolution, getting good coating uniformity across the mirror surface, and remounting the mirror equipped with the MFDs onto the Invar frame without altering the WFE as measured after polishing.

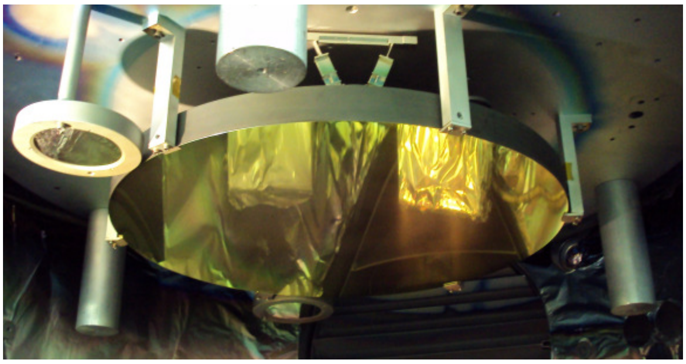

Figure 11. Mirror coated, in the coating chamber.

The following table summarizes the results achieved by implementing these different optimizations:

Parameters	Expectations	Measurements	Comments
Wave front error	30 nm RMS	**40 nm RMS**	The main residual effects are edge effects. If analyzed on a diameter reduced of 5% the WFE becomes compliant to the expectation.
Effect of the mounting/ dismounting on WFE	<10 nm RMS	**Negligible on the measured WFE RMS value**	Actually some residual effect can been seen when subtracting the two WFE maps. These residual effects are explained by the locating devices on the frame and can be enhanced.
Micro-roughness	< 10 nm RMS	**8 nm RMS**	The micro-roughness has been finalized in further polishing steps after WFE optimization.
Effect of the gold coating on WFE	About 1.8 nm RMS at room temperature	**Negligible**	Cannot be detected within the measurement accuracy, and further to the dismounting/ remounting residual effects.

The micro-roughness achieved on samples 100 mm in diameter was locally as low as 2.8 nm RMS. According to our experience, with further polishing, the same micro-roughness can be reached on the ULT mirror.

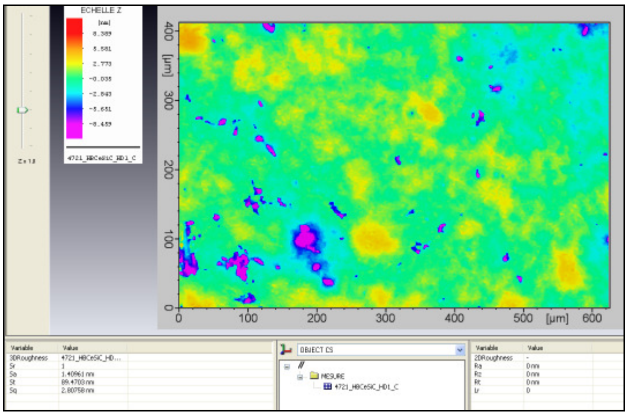

Variable	Value
3DRoughness	4721_HBCeSiC_HD...
Sr	1
Sa	1.40961 nm
St	89.4703 nm
Sq	2.80758 nm

Variable	Value
2DRoughness	-
Ra	0 nm
Rz	0 nm
Rt	0 nm
Lr	0

Figure 12. Micro-roughness measured on a Ø100 mm sample (2.8 nm RMS).

5. DISCRIPTION OF THE CRYO TEST FACILITY AND TEST PARAMETERS

The testing of the ULT mirror's SFE at cryogenic temperatures was performed at the TAS Optical Test Center, Cannes, France.

For the optical test, the mirror was fixed on an Invar frame located inside a thermal shroud, cooled to liquid N_2 temperature, located on an optical bench in a thermal vacuum chamber at ambient temperature. External to the cryo chamber, a fast ZYGO interferometer was used to illuminate through a lens the mirror and measure its surface at the center of curvature.

Such an optical test set-up offers a high accuracy as transmission flat and focus lens are inside the chamber at ambient temperature, and it gives a very high reproducibility. A removable reference calibration sphere, made of Zerodur and positioned at each measurement point between the mirror and focus lens, allows the suppression of all optical artifacts generated independently of the mirror surface (lens, window, flat, etc.) and produces a very low noise level (the bench being suspended and the entire configuration located on an antiseismic block).

The test set-up for the cryo cool-down consisted of four thermal N_2 cryo shrouds, ensuring a uniform temperature of the mirror and a thermal coupling between Invar frame and cryo shrouds.

A relative accuracy budget between two measurements was established and confirmed by repeatability measurements done on the test set-up.

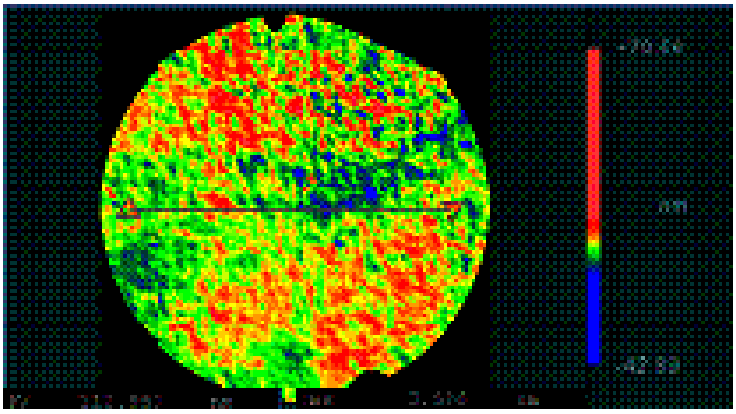

Figure 13. WFE measurement reproducibility to better than 4 nm RMS.

6. RESULTS OF THE CRYO TEST

The mirror WFE evolution was precisely measured between ambient and cryo temperatures through an exhaustive test sequence. For each temperature, the mirror WFE was measured 10 times; the average value was computed; and a map of the data was generated.

First, the WFE of the mirror was measured without the ACD at ambient temperature under vacuum, then at cryo temperature at 93 K and finally at ambient under vacuum after the cryo test.

This measurement showed a very low WFE increase, namely, 17 nm RMS from 91 nm RMS.

By subtracting one map from the other, we obtained the "ΔWFE" and determined the impact of the cryogenic conditions on the mirror WFE. The ΔWFE map at cryo is the results of different phenomena:

- Impact of reflective cladding, Invar fixations, glue, and Invar frame due to the CTE mismatches.
- Impact of small inhomogeneities of the HB-Cesic® material of the mirror structure.

Using precise FEM of the whole equipped mirror on its frame, the mirror WFE evolution during the cryo test was predicted using material data and DL/L data from 300 K to 93 K, mirror core being considered with uniform HB-Cesic® CTE .

When we compare the predicted WFE map with the measured one, we observe the same WFE map shape and the same level of ΔWFE between prediction and measurement. This excellent correlation is an indicator of the high homogeneity of the HB-Cesic® mirror.

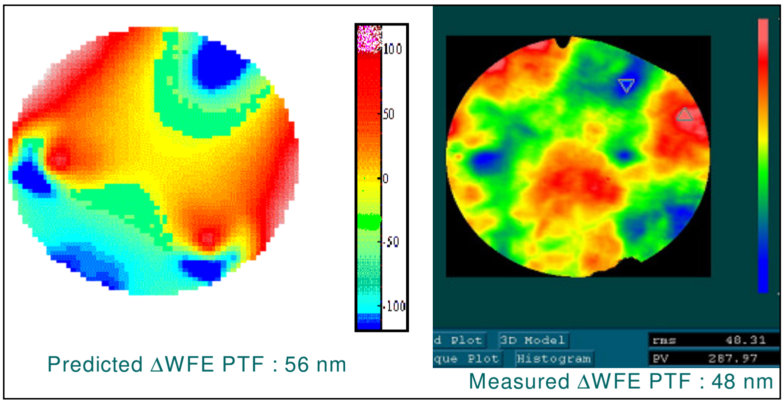

Predicted ΔWFE PTF : 56 nm

Measured ΔWFE PTF : 48 nm

Figure 14. Illustration of the very high correlation between prediction and measured WFE map.

Comparing the high-frequency WFE terms gives the same level of ΔWFE as for the lower-frequency terms**.** This indicates the high reliability of the FEM prediction vs. the measurements and, therefore, the high homogeneity of the HB-Cesic® material.

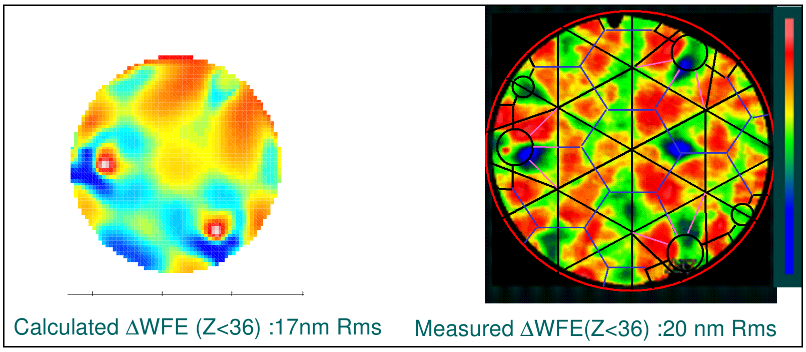

Calculated ΔWFE (Z<36) :17nm Rms

Measured ΔWFE(Z<36) :20 nm Rms

Figure 15. Illustration of the very high correlation between prediction and measured WFE (Z<36) for high-frequency terms.

There exists some correlation between the ΔWFE (Z<36) map and the rib pattern, showing a very small thermo-elastical cell quilting (around 10 nm) .

After the cryo test, the mirror WFE was measured again, this measurement indicated that the WFE is very stable before and after the cryo test, with WFE values of 91.45 nm RMS and 91.46 nm RMS, respectively.

Even for high-frequency terms (Z>36) no change in ΔWFE was measured.

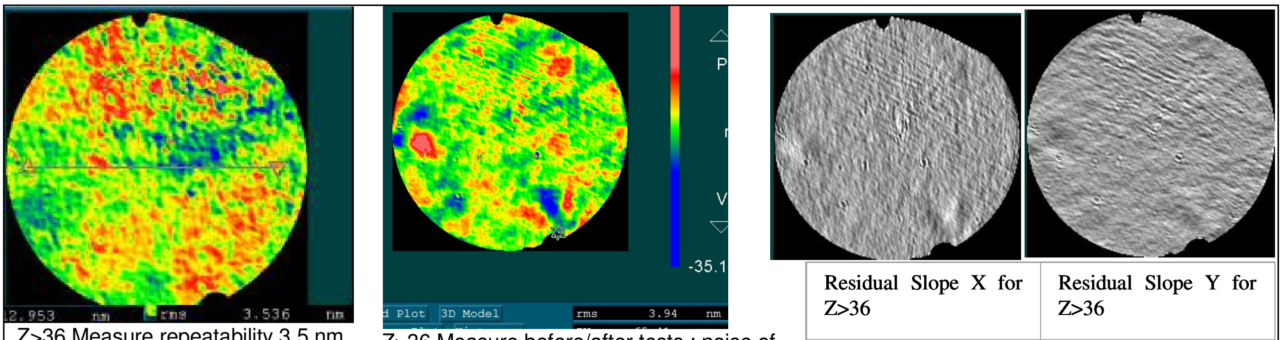

Z>36 Measure repeatability 3,5 nm Rms pure noise

Z>36 Measure before/after tests : noise of repeatability + I/f fixation impact : 3,9 nm Rms

Residual Slope X for Z>36

Residual Slope Y for Z>36

Figure 16. WFE (Z<36) map evolution 3.9 nm vs. noise level 3.5 nm.

These measurements demonstrate that the ULT HB-Cesic® mirror is very stable at the nm-level before and after the cryo test.

After completion of this successful test, the mirror was integrated with the ACD beam. The WFE of the mirror was then measured at ambient temperature and, finally, at cryo temperature with and without activation of the ACD. Integration of the ACD did not degrade the mirror WFE. For instance, the WFE had a value of 126 nm RMS after integration compared to 127 nm RMS before.

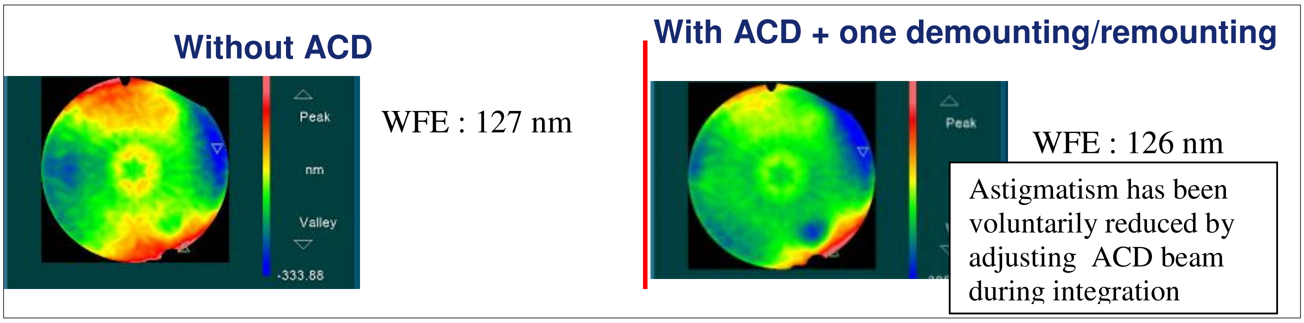

Without ACD

WFE : 127 nm

With ACD + one demounting/remounting

WFE : 126 nm

Astigmatism has been voluntarily reduced by adjusting ACD beam during integration

Figure 17. Very low WFE evolution due to ACD integration.

The ACD was activated at ambient with the mirror in front of the interferometer. We then measured the WFE and astigmatism evolution as a function of the temperature difference between the mirror and ACD at 293 K.

We observed a linear behavior and a perfect correlation with predictions for the astigmatism term and also for the residual terms. We observed no residual terms after the temperature of the ACD had returned to that of the mirror.

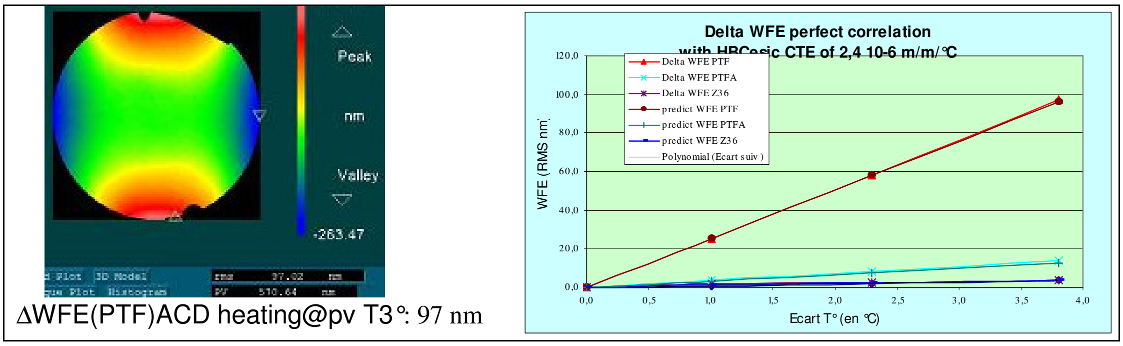

ΔWFE(PTF)ACD heating@pv T3°: 97 nm

Figure 18. WFE performance at ambient temperature during activation of the ACD.

After ACD activation, the mirror and ACD beam were cooled to 100 K.

After the mirror and ACD had become stabilized at cryo temperature, we measured the ΔWFE (cryo/ambient) and compared the results with prediction. Measurements and prediction were very close. [Predicted ΔWFE (ambient-100K) was 75 nm RMS vs. a measured ΔWFE of 106 nm RMS.]

The ΔWFE maps show close agreement between predictions and measurements.

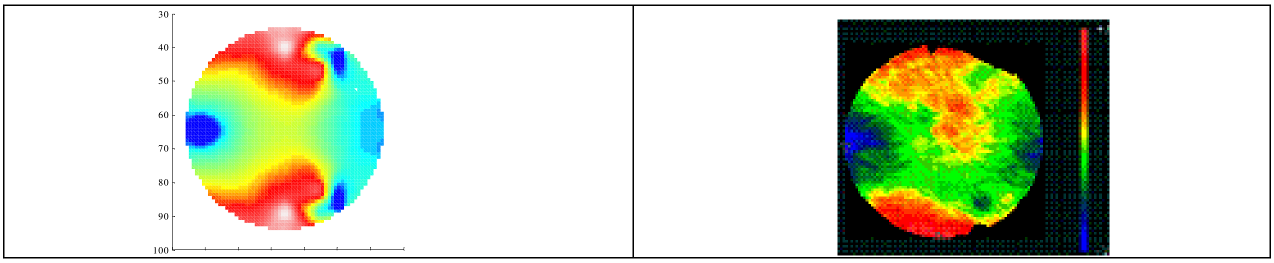

Figure 19. Map comparison of mirror plus ACD at cryo temperature (left) and ΔWFE at cryo/ambient (right).

We measured the mirror WFE with the ACD activated at cryo temperature for different ACD temperatures. As predicted, we obtained a quasi-pure astigmatism.

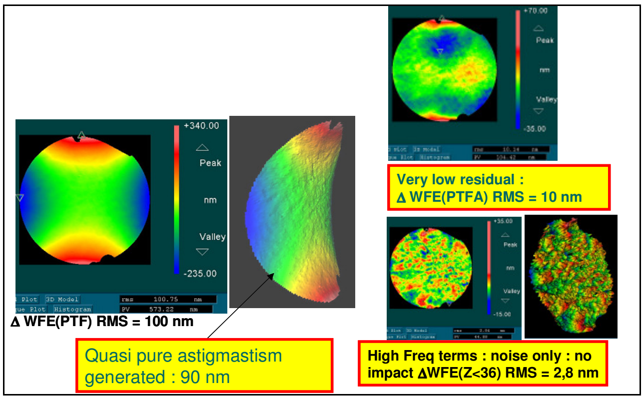

Δ WFE(PTF) RMS = 100 nm

Quasi pure astigmastism generated : 90 nm

Very low residual :
Δ WFE(PTFA) RMS = 10 nm

High Freq terms : noise only : no impact ΔWFE(Z<36) RMS = 2,8 nm

Figure 20. Mirror WFE when ACD is activated at cryo.

We measured the mirror WFE evolution as a function of the ACD temperature after the ACD had been activated at cryo temperature and compared the results with predictions There existed a perfect correlation between the measured WFE (PTF, PTFA, and Z<36) vs. ACD heating vs. predicted values at cryogenic temperature. We also noticed a very close correlation in the WFE maps between prediction and measurements while the ACD was activated.

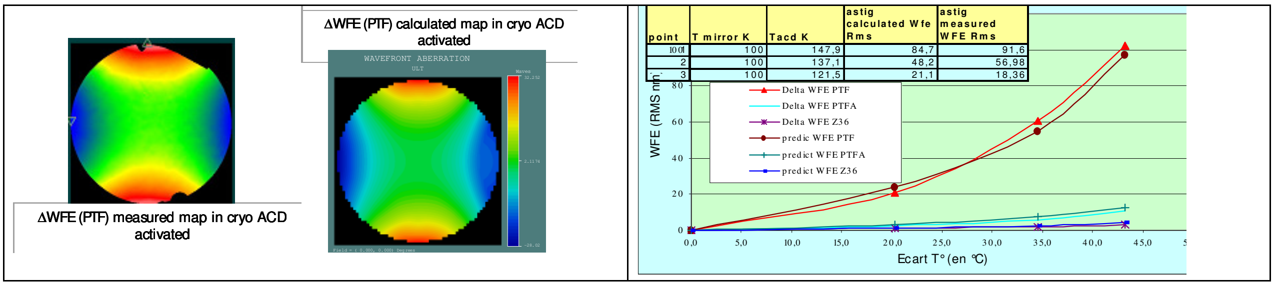

point	T mirror K	Tacd K	astig calculated Wfe Rms	astig measured WFE Rms
1	100	147,9	84,7	91,6
2	100	137,1	48,2	56,98
3	100	121,5	21,1	18,36

Figure 21. Mirror WFE and WFE (A) evolution as a function of temperature.

Thanks to very precise WFE measurements, this intensive test campaign has allowed us to unambiguously demonstrate the very stable behavior of the HB-Cesic® mirror from ambient to a cryo temperature of 93 K and the perfect performance of the ACD beam in correcting for any astigmatism at ambient and at cryo temperatures.

7. CONCLUSION

Based on our successful ULT optical mirror development, we can state with confidence that the HB-Cesic® technology has reached maturity and is suitable, with very little risk, for large, ultra-lightweighted future space optics applications at cryogenic temperatures.

Our mirror demonstration project showed the following capabilities:

- Construction of a 600-mm mirror with an areal density of 17 kg/m^2 and possessing high stiffness and high strength.
- High polishing quality of the mirror to a surface error of 20 nm P-V, with the possibility of further improvements.

Our highly accurate and exhaustive cryogenic WFE test campaign demonstrated:

- Outstanding performance at cryo temperatures of the HB-Cesic® mirror.
- Highly accurate WFE prediction consistent with all of the measurements.
- Very high performance of the ACD beam.

We achieved all of the project requirements – such as mirror mass, mirror optical performance, and mirror-ACD cryogenic performance. Furthermore, we demonstrated with our accurate CAD design and FEM analysis the ability to achieve a very high level of correlation between the test results and modeling, which is fully compatible including margins and extrapolation through FEM analysis to large-size mirrors with the specifications of the SPICA and Darwin missions.